2,2′-Bipyrimidine as Efficient Sensitizer of the Solid-State Luminescence of Lanthanide and Uranyl Ions from Visible to Near-Infrared

ARTICLE *in* CHEMISTRY - A EUROPEAN JOURNAL · SEPTEMBER 2009

Impact Factor: 5.73 · DOI: 10.1002/chem.201090004 · Source: PubMed

6 AUTHORS, INCLUDING:

Gaël Zucchi
École Polytechnique
28 PUBLICATIONS **699** CITATIONS
SEE PROFILE

Olivier Maury
Ecole normale supérieure de Lyon
169 PUBLICATIONS **3,431** CITATIONS
SEE PROFILE

Jean-Claude G Bünzli
École Polytechnique Fédérale de Lausanne
482 PUBLICATIONS **16,884** CITATIONS
SEE PROFILE

CHEMISTRY
A EUROPEAN JOURNAL

DOI: 10.1002/chem.200901517

2,2′-Bipyrimidine as Efficient Sensitizer of the Solid-State Luminescence of Lanthanide and Uranyl Ions from Visible to Near-Infrared

Gaël Zucchi,*[a] Olivier Maury,[b] Pierre Thuéry,[a] Frédéric Gumy,[c] Jean-Claude G. Bünzli,[c] and Michel Ephritikhine[a]

Abstract: Treatment of $Ln(NO_3)_3{\cdot}nH_2O$ with 1 or 2 equiv 2,2′-bipyrimidine (BPM) in dry THF readily afforded the monometallic complexes $[Ln(NO_3)_3(bpm)_2]$ (Ln = Eu, Gd, Dy, Tm) or $[Ln(NO_3)_3(bpm)_2]{\cdot}THF$ (Ln = Eu, Tb, Er, Yb) after recrystallization from MeOH or THF, respectively. Reactions with nitrate salts of the larger lanthanide ions (Ln = Ce, Nd, Sm) yielded one of two distinct monometallic complexes, depending on the recrystallization solvent: $[Ln(NO_3)_3(bpm)_2]{\cdot}THF$ (Ln = Nd, Sm) from THF, or $[Ln(NO_3)_3(bpm)(MeOH)_2]{\cdot}MeOH$ (Ln = Ce, Nd, Sm) from MeOH. Treatment of $UO_2(NO_3)_2{\cdot}6H_2O$ with 1 equiv BPM in THF afforded the monoadduct $[UO_2(NO_3)_2(bpm)]$ after recrystallization from MeOH. The complexes were characterized by their crystal structure. Solid-state luminescence measurements on these monometallic complexes showed that BPM is an efficient sensitizer of the luminescence of both the lanthanide and the uranyl ions emitting visible light, as well as of the Yb^{III} ion emitting in the near-IR. For Tb, Dy, Eu, and Yb complexes, energy transfer was quite efficient, resulting in quantum yields of 80.0, 5.1, 70.0, and 0.8%, respectively. All these complexes in the solid state were stable in air.

Keywords: bipyrimidine · lanthanides · luminescence · sensitizers · solid-state structures

Introduction

Their seven f orbitals confer upon trivalent lanthanide ions electronic properties leading to intrinsic physical properties which are very attractive for the development of new materials with potential applications in various domains, from medicine and biology to materials science for new technologies. In particular, they are paramagnetic (except for La^{3+} and Lu^{3+}), and the discovery of a ferromagnetic interaction between Gd^{III} and Cu^{II}[1] has encouraged continuously expanding research on their utility and performance in the field of (molecular) magnetism.[2] Another important field of thorough investigation involving lanthanides is the application of their luminescence properties. Emission from the trivalent lanthanide ions (except Ce^{3+}) originates from a rearrangement of the electrons within the 4f subshell, and the transitions are parity-forbidden. Consequently the emission lines are very sharp (full-width at half-height a few nanometers) and the excited-state lifetimes are relatively long (usually within the micro- to millisecond range, depending on the ion). These properties allow time-resolved experiments to be used as very powerful analysis tools in bioinorganic chemical applications such as fluoroimmunoassays and protein labeling.[3–10] The long excited-state lifetimes and the high chromaticity of lanthanides are also interesting for applications in solid-state materials technologies. For instance, Tb^{3+}, Eu^{3+}, and Tm^{3+} are used as green, red, and blue emitters in, respectively, trichromatic fluorescent tubes, multicolor displays,[11,12] and organic light-emitting diodes (OLEDs).[13,14] Dy^{3+} is found in persistent-luminescence phosphors as these materials do not need radioactive ions such as ^3H or ^{147}Pm to sustain their phosphorescence.[15] The near-IR emitters Nd^{3+}, Yb^{3+}, and Er^{3+} are of special interest in photonics, being used as laser-active dopants in a variety of host materials, including both crystals and glasses.[16,17] Er^{3+} is of interest for use as a planar-waveguide optical amplifier, as it emits at 1.5 μm, one of the standard telecommunication wavelengths.[18–20]

For most of the solid-state applications described above, the lanthanide ion is usually incorporated as a dopant in a host inorganic matrix. However, continuous efforts are being made to develop new air-stable and highly luminescent materials with satisfactory mechanical, thermal, and chemical stability that can be easily processed. Along these lines, sol–gel chemistry has proven to be useful for the development of interesting photoluminescent materials in which the lanthanide ions are embedded in porous silicate glasses.[21–27] Coordination polymers are another family of materials that combine the physicochemical properties of organic molecules with the physical properties of the metal ions. These edifices, in which an organic ligand is used as a linker to connect metal ions, have emerged as a new class of potential materials for functions such as gas storage, exchange, separation, and catalysis.[28–34] In particular, because they have large ionic radii and luminescent properties, f elements give rise to a wealth of metal–organic frameworks with structural diversity and interesting emissive properties.[35–43] The synthesis of these materials requires a precise knowledge of the structure and behavior of the components, especially the key role of the organic linker in the structural assembly and the physicochemical properties. We have recently described the synthesis, structure, and luminescence properties of neodymium–bipyrimidine compounds with nitrate and various β-diketonate ligands.[44] In these com-

[a] Dr. G. Zucchi, Dr. P. Thuéry, Dr. M. Ephritikhine
CEA, IRAMIS, SIS2M, Laboratoire Claude Fréjacques
CNRS URA 331, 91191 Gif-sur-Yvette (France)
Fax: (+33) 169-08-66-40
E-mail: gael.zucchi@cea.fr

[b] Dr. O. Maury
Université de Lyon, Laboratoire de Chimie
CNRS-Ecole Normale Supérieure de Lyon
UMR 5182, 46 allée d'Italie, 69007 Lyon (France)

[c] F. Gumy, Prof. Dr. J.-C. G. Bünzli
Laboratory of Lanthanide Supramolecular Chemistry
École Polytechnique Fédérale de Lausanne (EPFL), 1015 Lausanne (Switzerland)

Supporting information for this article is available on the WWW under http://dx.doi.org/10.1002/chem.200901517.

plexes, which exhibit a remarkable structural diversity from mono- and binuclear species to metal–organic frameworks, the BPM connecting ligand plays an important role in the process of sensitization of Nd^{III} luminescence. Herein, we report structural and photophysical investigations on simple systems made only of an f element, nitrate, and BPM. In particular, we point out the double role of BPM as a ligand for the lanthanide- and uranyl-ion series and as a sensitizer of their luminescence.

Results and Discussion

Synthesis and crystal structure of the complexes: Recently we reported that treatment of $Nd(NO_3)_3{\cdot}6H_2O$ with 1 equiv BPM in THF led to precipitation of an off-white powder which was recrystallized from methanol to give pale purple crystals of the mono- BPM adduct $[Nd(NO_3)_3(bpm)(MeOH)_2]{\cdot}MeOH$ in 48% yield.[44] Since then, we have found that a THF solution of a 1:2 mixture of $Nd(NO_3)_3{\cdot}6H_2O$ and BPM deposited crystals suitable for X-ray diffraction of the bis adduct $[Nd(NO_3)_3(bpm)_2]{\cdot}THF$ in 65% yield. Crystals of the cerium and samarium counterparts $[Ln(NO_3)_3(bpm)(MeOH)_2]{\cdot}MeOH$ (Ln = Ce, Sm) and $[Sm(NO_3)_3(bpm)_2]{\cdot}THF$ were obtained in a similar way. However, reactions of the nitrate salts of the heavier lanthanide ions with BPM in THF or methanol afforded crystals of only the bis adducts $[Ln(NO_3)_3(bpm)_2]{\cdot}THF$ (Ln = Nd, Sm, Eu, Tb, Er, Yb) or $[Ln(NO_3)_3(bpm)_2]$ (Ln = Eu, Gd, Dy, Tm), respectively. These compounds are rare examples of lanthanide complexes with BPM as a terminal ligand and, with the recently reported $[Tb(hfac)_3(bpm)(H_2O)]$ compound (hfac = hexafluoroacetylacetonate anion),[45] they are the only mononuclear lanthanide compounds comprising BPM to have been characterized crystallographically. The synthesis of $[Ln(NO_3)_3(bpm)_2]{\cdot}THF$ (Ln = Eu, Tb) contrasts with that of the corresponding dinuclear complexes $[\{Ln(NO_3)_3(bpm)\}_2(\mu\text{-bpm})]$, which were reported to be the only isolable products from the $Ln(NO_3)_3{\cdot}6H_2O$/BPM reaction system, whatever the reagent ratio, the solvent, and the crystallization method used.[46] Our attempts to reproduce the preparation of these dinuclear compounds were unsuccessful, invariably giving the mononuclear complexes. The synthesis of $[Ln(NO_3)_3(bpm)(MeOH)_2]$ (Ln = Ce, Nd and Sm) indicates that MeOH does not displace a BPM ligand from the $[Ln(NO_3)_3(bpm)_2]$ complexes of the heavier lanthanides. This feature is likely related to the fact that the BPM ligand is more tightly bound to the more Lewis-acidic metal ions.[47]

The crystal structures of $[Ln(NO_3)_3(bpm)(MeOH)_2]{\cdot}MeOH$ (Ln = Ce, Sm) are isomorphous with that of the neodymium analogue that has already been described,[44] and will not be mentioned further. Figure 1 shows a view of the cerium derivative and selected bond lengths and angles are listed in Table 1. The bond lengths decrease in the order Ce > Nd > Sm, reflecting the variation in the radii of the Ln^{3+} ions.[48]

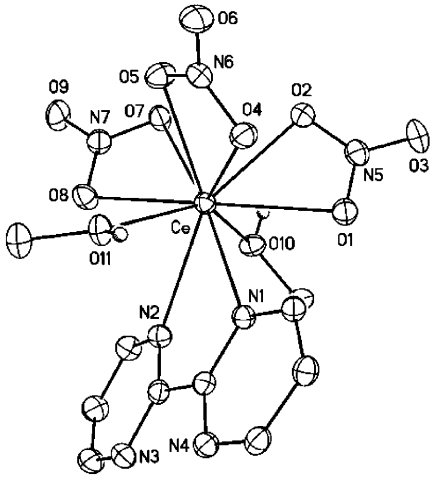

Figure 1. View of the Ce^{III} complex, representative of the isomorphous $[Ln(NO_3)_3(bpm)(MeOH)_2]$ (Ln = Ce, Nd, Sm) series. Hydrogen atoms of the BPM ligand are omitted. Displacement ellipsoids are drawn at the 50% probability level.

Table 1. Selected bond lengths [Å] and angles [°] for the complexes $[Ln(NO_3)_3(bpm)(MeOH)_2]{\cdot}MeOH$ (Ln = Ce, Nd, Sm). Averages are given in angle brackets.

Ln	Ce	Nd	Sm
Ln–O1	2.5606(18)	2.5256(18)	2.503(2)
Ln–O2	2.5716(18)	2.5366(18)	2.516(2)
Ln–O4	2.5415(17)	2.5047(18)	2.470(2)
Ln–O5	2.5934(19)	2.557(2)	2.536(3)
Ln–O7	2.5937(17)	2.5673(17)	2.550(2)
Ln–O8	2.6102(19)	2.5737(19)	2.543(2)
⟨Ln–O(NO$_3$)⟩	2.58(2)	2.54(2)	2.52(3)
Ln–O10	2.5176(18)	2.4856(19)	2.455(2)
Ln–O11	2.5129(17)	2.4855(18)	2.452(2)
Ln–N1	2.690(2)	2.655(2)	2.625(2)
Ln–N2	2.681(2)	2.645(2)	2.614(2)
⟨Ln–N⟩	2.685(6)	2.650(7)	2.619(8)
N1-Ln-N2	60.51(6)	61.31(6)	61.80(7)
O1-Ln-O2	49.96(6)	50.67(6)	51.11(7)
O4-Ln-O5	50.09(5)	50.78(6)	51.35(7)
O7-Ln-O8	49.09(5)	49.72(5)	50.37(6)

The complexes $[Ln(NO_3)_3(bpm)_2]$ (Ln = Eu, Gd, Dy, Tm) and the THF solvates $[Ln(NO_3)_3(bpm)_2]{\cdot}THF$ (Ln = Nd, Eu, Tb, Er, Yb) are isostructural, the structures in each series being isomorphous. Figure 2 shows a view of the neodymium compound and selected bond lengths and angles are listed in Tables 2 and 3 (THF solvates).

The structure resembles that of the 2,2′-bipyridine (BIPY) analogues $[Ln(NO_3)_3(bipy)_2]$;[49,50] the environment of the 10-coordinate metal can be seen as a slightly distorted bicapped square antiprism, with the square faces defined by the N1, N5, O2, O4 and N2, N6, O5, O7 atoms, and with the O1 and O8 atoms in capping positions. The average Ln–O(NO$_3$) and Ln–N distances in $[Ln(NO_3)_3(bpm)_2]$ (Ln = Nd, Sm) are similar to those measured in $[Ln(NO_3)_3(bpm)(MeOH)_2]$. The Ln–O distances are also similar to those found in $[Ln(NO_3)_3(bipy)_2]$, whereas the Ln–N distances

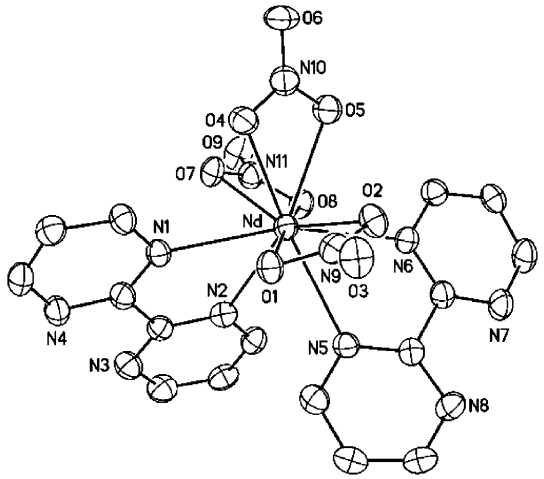

Figure 2. View of the Nd^{III} complex, representative of the isostructural $[Ln(NO_3)_3(bpm)_2]$ (Ln = Nd, Sm, Eu, Gd, Tb, Dy, Er, Tm, Yb) series. Hydrogen atoms are omitted. Displacement ellipsoids are drawn at the 50% probability level.

Table 2. Selected bond lengths [Å] and angles [°] for the complexes $[Ln(NO_3)_3(bpm)_2]$ (Ln = Eu, Gd, Dy, Tm). Averages are given in angle brackets.

Ln	Eu	Gd	Dy	Tm
Ln–O1	2.504(8)	2.503(2)	2.482(2)	2.456(3)
Ln–O2	2.517(8)	2.504(2)	2.4799(19)	2.447(3)
Ln–O4	2.473(8)	2.4611(19)	2.4354(19)	2.411(2)
Ln–O5	2.485(8)	2.468(2)	2.445(2)	2.418(3)
Ln–O7	2.454(8)	2.436(2)	2.4077(19)	2.375(3)
Ln–O8	2.536(9)	2.514(2)	2.495(2)	2.473(3)
⟨Ln–O⟩	2.49(3)	2.48(3)	2.46(3)	2.43(3)
Ln–N1	2.581(9)	2.568(2)	2.543(2)	2.515(3)
Ln– N2	2.556(10)	2.556(2)	2.523(2)	2.487(3)
Ln–N5	2.601(10)	2.600(2)	2.574(2)	2.539(3)
Ln–N6	2.632(10)	2.616(2)	2.591(2)	2.565(3)
⟨Ln–N⟩	2.59(3)	2.58(3)	2.56(3)	2.53(3)
N1-Ln-N2	62.9(3)	63.20(7)	63.86(7)	64.49(10)
N5-Ln-N6	62.0(3)	62.00(8)	62.48(7)	63.08(10)
O1-Ln-O2	51.3(3)	51.24(7)	51.81(7)	52.14(9)
O4-Ln-O5	51.9(3)	52.21(6)	52.65(6)	53.21(8)
O7-Ln-O8	51.8(3)	51.63(6)	52.24(6)	52.70(9)

appear to be shorter by 0.03–0.05 Å than the corresponding distances in the BIPY analogues. This difference between the Ln–N(bpm) and Ln–N(bipy) distances could be related to the weaker Lewis basicity of the BPM than of the BIPY ligand. The usual linear relationship holds between the Ln–O and Ln–N distances and the radii of the Ln^{3+} ions, with r^2 coefficients larger than 0.99.

Yellow crystals of $[UO_2(NO_3)_2(bpm)]$ were obtained from a 1:1 mixture of $UO_2(NO_3)_2{\cdot}6H_2O$ and BPM in dry THF by layering pentane. Figure 3 shows a view of the complex and

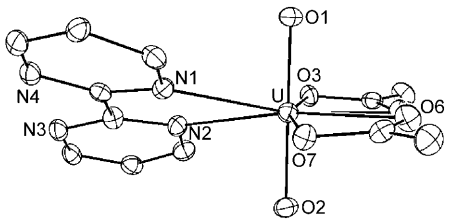

Figure 3. View of $[UO_2(NO_3)_2(bpm)]$. Hydrogen atoms are omitted. Displacement ellipsoids are drawn at the 50% probability level.

selected bond lengths and angles are presented in Table 4. The structure is identical to that adopted by the BIPY and 1,10-phenanthroline (PHEN) analogues,[51,52] with no significant difference in the corresponding U–O and U–N distan-

Table 4. Selected bond lengths [Å] and angles [°] for the complex $[UO_2(NO_3)_2(bpm)]$.

U–O1	1.766(5)	U–O2	1.769(5)
U–O3	2.494(5)	U–O4	2.467(5)
U–O6	2.478(6)	U–O7	2.496(5)
U–N1	2.566(6)	U–N2	2.584(7)
O1-U-O2	179.5(3)	O3-U-O4	51.37(18)
O6-U-O7	51.46(18)	N1-U-N2	62.96(19)

Table 3. Selected bond lengths [Å] and angles [°] for the complexes $[Ln(NO_3)_3(bpm)_2]{\cdot}THF$ (Ln = Nd, Sm, Eu, Tb, Er, Yb). Averages are given in angle brackets.

Ln	Nd	Sm	Eu	Tb	Er	Yb
Ln–O1	2.538(2)	2.515(3)	2.502(4)	2.495(2)	2.4618(17)	2.444(2)
Ln–O2	2.526(3)	2.503(4)	2.483(5)	2.461(2)	2.4293(18)	2.416(3)
Ln–O4	2.508(2)	2.477(4)	2.465(4)	2.445(2)	2.4079(16)	2.3961(18)
Ln–O5	2.519(3)	2.486(4)	2.468(4)	2.452(2)	2.4181(17)	2.4081(18)
Ln–O7	2.533(3)	2.507(4)	2.493(4)	2.465(2)	2.4398(18)	2.427(2)
Ln–O8	2.543(2)	2.520(3)	2.508(4)	2.497(2)	2.4651(17)	2.450(2)
⟨Ln–O⟩	2.527(13)	2.501(16)	2.486(17)	2.47(2)	2.44(2)	2.42(2)
Ln–N1	2.622(3)	2.602(4)	2.592(5)	2.567(2)	2.531(2)	2.510(2)
Ln–N2	2.619(3)	2.591(4)	2.581(6)	2.552(3)	2.519(2)	2.506(3)
Ln–N5	2.639(3)	2.605(4)	2.601(5)	2.568(2)	2.530(2)	2.517(2)
Ln–N6	2.627(3)	2.607(4)	2.599(5)	2.569(2)	2.5434(19)	2.523(2)
⟨Ln–N⟩	2.626(8)	2.601(7)	2.593(9)	2.564(8)	2.531(10)	2.514(7)
N1-Ln-N2	61.43(9)	61.92(13)	62.21(17)	62.84(8)	63.55(7)	63.95(8)
N5-Ln-N6	61.48(9)	62.27(13)	62.28(15)	63.07(8)	63.73(6)	63.90(7)
O1-Ln-O2	50.73(8)	51.41(11)	51.73(14)	51.68(7)	52.41(6)	52.63(7)
O4-Ln-O5	51.16(8)	51.63(12)	52.24(14)	52.33(7)	53.14(6)	53.36(6)
O7-Ln-O8	50.46(8)	50.92(11)	51.32(14)	51.51(7)	52.25(6)	52.57(7)

ces. The angle (23.74(10)°) between the plane of the BPM ligand and the mean equatorial plane of the complex is also identical to that observed in the BIPY compound.

These BPM complexes of the lanthanide and uranyl ions are air-stable in the solid state but decompose partially in solution, mainly because of ligand-exchange reactions with molecules of water. Thus, evaporation in air of methanol solutions of $[Ce(NO_3)_3(bpm)(MeOH)_2]$ and $[Yb(NO_3)_3(bpm)_2]$ led to the formation of crystals of $[Ce(NO_3)_2(bpm)(H_2O)_4][Ce(NO_3)_4(bpm)(H_2O)_2]$ and $[Yb(NO_3)_2(bpm)(H_2O)_3][NO_3]\cdot BPM\cdot 4H_2O$, respectively. Figure 4 shows a

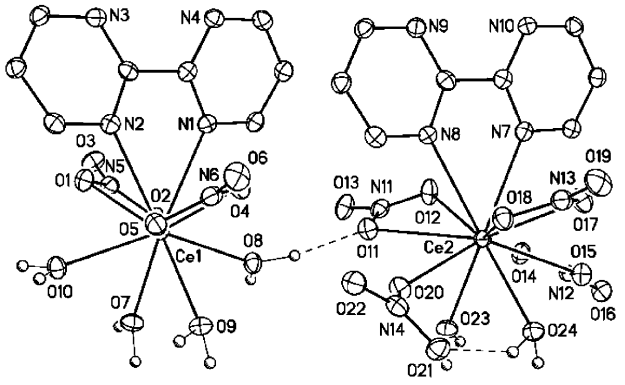

Figure 4. View of $[Ce(NO_3)_2(bpm)(H_2O)_4]^+[Ce(NO_3)_4(bpm)(H_2O)_2]^-$. Displacement ellipsoids are drawn at the 50% probability level.

view of the cerium compound and selected bond lengths and angles are listed in Table S1 (Supporting Information). The complex is built up of cation–anion pairs. Numerous hydrogen bonds between the water ligands and either nitrate oxygen atoms or BPM nitrogen atoms are present in the packing. The nitrate ligands are bidentate except for one on the anion, around N14, which is monodentate and linked by a hydrogen bond to an adjacent H_2O molecule. The structure of the cation is similar to that determined in the 3D supramolecular systems $[Ln(NO_3)_2(bpm)(H_2O)_4][Fe(CN)_4(bipy)]$ (Ln = Pr, Nd, Sm, Gd).[53] The average Ce1–$O(NO_3)$, Ce1–$O(H_2O)$, and Ce1–N distances (2.62(9), 2.49(2), and 2.74(3) Å, respectively) are comparable with the corresponding distances in the praseodymium cation (2.62(10), 2.47(1), and 2.774(3) Å). The structure is also similar to that of $[La(NO_3)_2(phen)(H_2O)_4]^+$;[54] the average Ce1–$O(NO_3)$ and Ce1–$O(H_2O)$ distances of 2.62(9) and 2.49(2) Å appear to be 0.05 Å shorter than the corresponding La–O distances, in agreement with the variation in the radii of the Ce^{3+} and La^{3+} ions,[48] whereas the Ce1–N distances are approximately 0.05 Å longer than the La–N distances, probably reflecting the weaker Lewis basicity of BPM than PHEN. The Ce2 atom in the anion $[Ce(NO_3)_4(bpm)(H_2O)_2]^-$ is 11-coordinate, like the metal centers in $[Pr(NO_3)_4(bipy)(H_2O)]^-$[55] and $[Ln(NO_3)_4(terpy)]^-$ (Ln = La,[56] Ce,[57] Sm[58]) in which all the nitrate ligands are bidentate. The Ce2–O20 distance corresponding to the monodentate nitrate ligand is 0.17 Å shorter than the average Ce2–O(κ^2-NO_3) distance; this feature was noted previously in the structures of the $[Ln(NO_3)_4(terpy)]^-$ anions (terpy = terpyridine)(Ln=Nd, Sm, Tb, Dy, Ho) in which a unique nitrate ligand is monodentate and the Ln atom is 10-coordinate.[59] Figure 5 shows a view

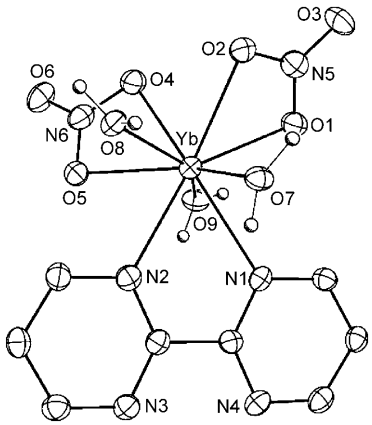

Figure 5. View of $[Yb(NO_3)_2(bpm)(H_2O)_3]^+$. Hydrogen atoms of the BPM ligand are omitted. Displacement ellipsoids are drawn at the 50% probability level.

of the cation $[Yb(NO_3)_2(bpm)(H_2O)_3]^+$ and selected bond lengths and angles are listed in Table S2 (Supporting Information). The Yb–$O(NO_3)$, Yb–$O(H_2O)$, and Yb–N distances are quite similar to those measured in $[Yb(NO_3)_2(terpy)(H_2O)_2]^+$.

Photophysical properties: In undried methanol at a millimolar concentration, $[Tb(NO_3)_3(bpm)_2]$ shows a relatively weak Tb-centered luminescence that almost completely disappears at a micromolar concentration. In contrast with the results described below for this complex in the solid state, the solution measurements indicate that decoordination of the BPM occurs in a coordinating solvent in the presence of water (Figure F1, Supporting Information). Therefore, we hereafter restrict the luminescence investigation to complexes conditioned as microcrystalline powders. Unless specified, measurements have been performed at room temperature. Excitation and emission spectra of the complexes comprising the visible-emitting lanthanide ions (Ln = Sm, Eu, Tb, Dy, Tm) are reported in Figure 6. Monitoring of the metal-ion emission lines resulted in excitation spectra which display the typical narrow f–f absorption bands of the Ln^{3+} ions as well as a broad band attributed to π–π* and/or n–π* transitions within the electronic states of the organic BPM ligand. The latter band extends from 375 nm to less than 250 nm with maxima at 326 and 275 nm. These spectra clearly indicate that emission from the metal ions is obtained through an energy transfer from the organic ligand. This is further ascertained by the emission spectrum of $[Tm(NO_3)_3(bpm)_2]$ recorded after excitation of BPM at 380 nm (Figure 7a): dips in the phosphorescence band of BPM match the f–f transitions of Tm^{III} from the $^1G_4$ (≈470 nm) and $^3F_2$

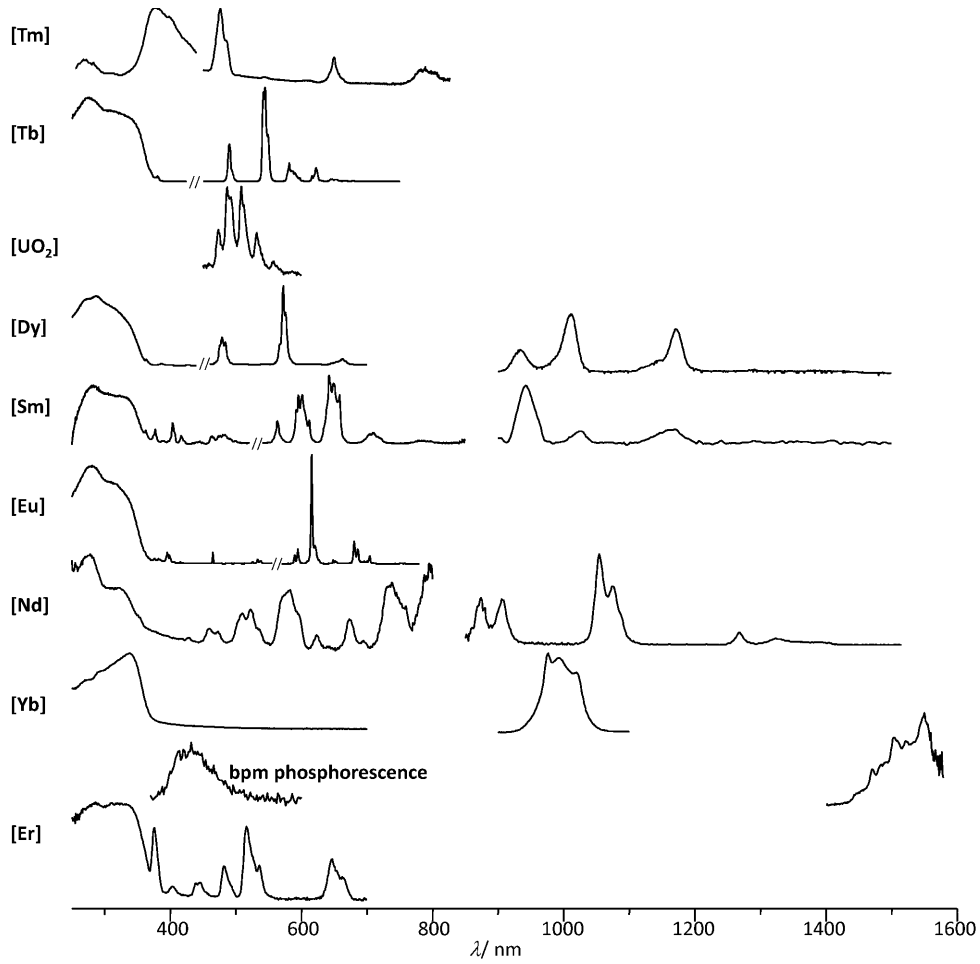

Figure 6. Excitation and emission spectra of the $[Ln(NO_3)_3(bpm)_2]$ complexes (Ln = Tm, Tb, Dy, Sm, Eu, Nd, Yb, Er) and $[UO_2(NO_3)_2(bpm)]$. Excitation spectra have been measured by monitoring the most intense band of the emission spectrum for each ion, and emission spectra have been obtained after excitation within the excited electronic states of BPM ($\lambda_{exc} = 330$ nm).

($\approx$650 nm) excited levels to the $^3H_6$ ground state; these transitions result in weak blue and red emission, respectively. However, phosphorescence of BPM is seen in the emission spectrum also (Figure 7b), indicating partial transfer only, probably due to back energy transfer from the Tm-($^1G_4$) level to the BPM levels because both emission spectra overlap in the 450–500 nm range.

Upon excitation of the BPM ligand at 330 nm, typical emission of each lanthanide investigated and of uranyl ions is observed, confirming energy transfer from BPM to the excited states of the metal ions. $[Sm(NO_3)_3(bpm)_2]$ emits orange light originating from the transitions $^4G_{5/2}\rightarrow{}^6H_{5/2}$ (563 nm), $^4G_{5/2}\rightarrow{}^6H_{7/2}$ (595 nm), $^4G_{5/2}\rightarrow{}^6H_{9/2}$ (645 nm), and $^4G_{5/2}\rightarrow{}^6H_{11/2}$ (711 nm). A lifetime of 47 μs was found for the $^4G_{5/2}$ level. Four of the $^5D_0\rightarrow{}^7F_J$ transitions of the red-emitting Eu^{III} ion are observed at 580 nm ($J=0$), between 590 and 594 nm ($J=1$), at 616 nm ($J=2$), between 646 and 655 nm ($J=3$), and between 671 and 715 nm ($J=4$), respectively. Excitation to the ligand levels at 270 nm yielded a monoexponential decay from which a lifetime of 1.31 ms was extracted. An intense green emission was observed for $[Tb(NO_3)_3(bpm)_2]$, with the typical $^5D_4\rightarrow{}^7F_J$ ($J=6$–2) transitions occurring at 490, 544, 582, 623, and 646 nm, respectively. The lifetime of the $^5D_4$ excited state amounts to 1.70 ms. The two $^4F_{9/2}\rightarrow{}^6H_{15/2,13/2}$ transitions of the Dy^{III} ion appear at 479 and 573 nm, respectively, the second one being more intense. This results in an overall yellow emission of the $[Dy(NO_3)_3(bpm)_2]$ complex. We have found a lifetime of 43 μs for the $^4F_{9/2}$ excited state. The typical structured emission band of the UO_2^{2+} ion is also observed in the green region between 465 and 575 nm after excitation of the BPM ligand in $[UO_2(NO_3)_2(bpm)]$. That no phosphorescence from BPM is observed in these visible-emitting complexes (except for $[Tm(NO_3)_3(bpm)_2]$, as described above) thus indicates a relatively efficient energy transfer from BPM to these ions.

This is confirmed by measurement of the quantum yields Φ (Table 5). Remarkably high values of 80.0 and 70.0% have been obtained for $[Tb(NO_3)_3(bpm)_2]$ and $[Eu(NO_3)_3(bpm)_2]$, respectively; they are among the highest values reported to date for molecular Tb^{III} and Eu^{III} complexes. Only a few Tb^{III} complexes have been reported to exhibit higher quantum yields in the solid state,[60] and only one Eu^{III} com-

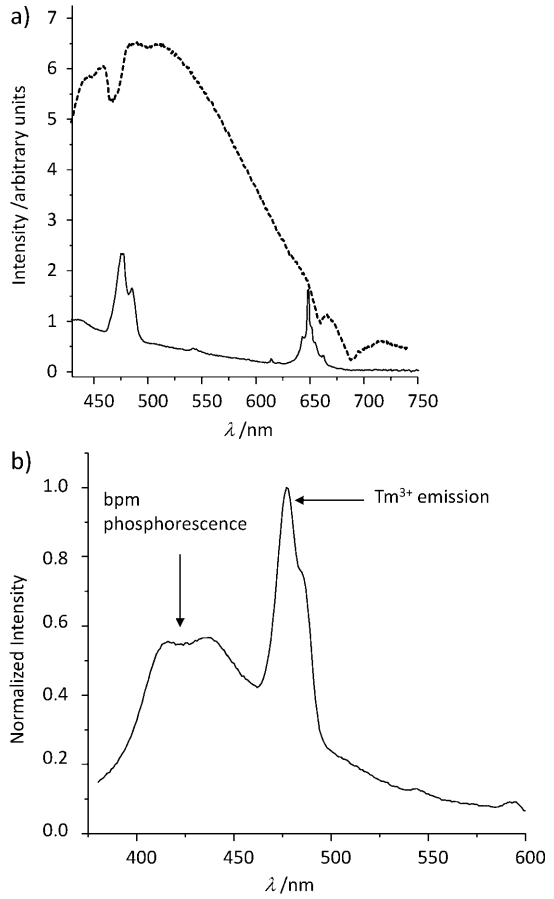

Figure 7. a) Emission spectra of $[Tm(NO_3)_3(bpm)_2]$ ($\lambda_{exc}=330$ nm, solid line; and $\lambda_{exc}=380$ nm, broken line); b) phosphorescence spectrum of $[Tm(NO_3)_3(bpm)_2]$ ($\lambda_{exc}=330$ nm).

Table 5. Experimental quantum yields measured in the solid state at 20°C (reproducibility given as $\pm 2\sigma$) and lifetimes of the $^5D_4$(Tb), $^5D_0$(Eu), $^4F_{9/2}$(Dy), and $^4G_{5/2}$(Sm) excited states.[a]

Complex[b]	Φ ($\pm 2\sigma$) [%]	τ [ms]
$[Tb(NO_3)_3(bpm)_2]$	80.0 ± 1.0	1.70 ± 0.01
$[Eu(NO_3)_3(bpm)_2]$	70.0 ± 1.0	1.31 ± 0.05
$[Dy(NO_3)_3(bpm)_2]$	5.1 ± 0.1	0.043 ± 0.005
$[Sm(NO_3)_3(bpm)_2]$	0.14 ± 0.02	0.047 ± 0.005
$[Sm(NO_3)_3(bpm)(CD_3OD)]$	0.09 ± 0.01	–
$[Yb(NO_3)_3(bpm)_2]$	0.8 ± 0.1	–

[a] Excitation wavelength: 336–338 nm for quantum yields and 270 nm for lifetimes. [b] Other complexes were too weakly luminescent for quantum-yield determination.

plex exhibits a higher quantum yield.[61] For comparison, by using the same equipment and technique, some of us recently reported a value of 72% for the tris(dipicolinate) complex, which is known to be highly luminescent.[62] That the energy transfer is quantitative in the Eu^{III} complex can be demonstrated by estimating its efficiency, η_{sens}, from Equations (1) and (2),[62] in which Φ_{Eu}^{L} and Φ_{Eu}^{Eu} are the overall (upon ligand excitation) and intrinsic (upon direct f–f excitation) quantum yields, n is the refractive index (about 1.5 for solid-state coordination compounds), and I_{tot} and I_{MD} are the integrated emission intensities of the entire spectrum and of the magnetic-dipole $^5D_0\rightarrow{}^7F_1$ transition, respectively. In our case, $I_{tot}/I_{MD}=10.1\pm0.3$, so that the radiative lifetime amounts to $\tau_{rad}=2.00\pm0.08$ ms, Φ_{Eu}^{Eu} is 66 ± 7% and therefore $\eta_{sens}\approx1$.

$$\Phi_{Eu}^{L}=\eta_{sens}\times\Phi_{Eu}^{Eu}=\eta_{sens}\times\frac{\tau_{obs}}{\tau_{rad}} \quad (1)$$

$$\frac{1}{\tau_{rad}}=14.65\times n^3\times\frac{I_{tot}}{I_{MD}}[s^{-1}] \quad (2)$$

An interesting value (5.1%) has also been recorded for $[Dy(NO_3)_3(bpm)_2]$. The quantum yields of the three Sm complexes, $[Sm(NO_3)_3(bpm)_2]$, $[Sm(NO_3)_3(bpm)(CD_3OD)_2]$, and $[Sm(NO_3)_3(bpm)(CH_3OH)_2]$ are consistent with nonradiative deactivation of the emissive $^4G_{5/2}$ excited state of the Sm^{III} ion by OH vibrations. The quantum yield could not be measured for the methanol solvate because the emission was too low, owing to the presence of two O–H oscillators in the first coordination sphere. Comparison of the values obtained for $[Sm(NO_3)_3(bpm)_2]$ (0.14%) and $[Sm(NO_3)_3(bpm)(CD_3OD)_2]$ (0.09%) shows that two molecules of BPM in the first coordination sphere lead to a more luminescent complex. We have observed emission in the near-IR from the Sm^{III} and Dy^{III} ions, which is a more rarely described phenomenon.[63,64] The three transitions $^4G_{5/2}\rightarrow{}^4F_{5/2}$ (943 nm), $^4G_{5/2}\rightarrow{}^4F_{7/2}$ (1024 nm), and $^4G_{5/2}\rightarrow{}^4F_{9/2}$ (1169 nm) are observed for $[Sm(NO_3)_3(bpm)_2]$ and emission bands with maxima at 933 ($^4F_{9/2}\rightarrow{}^6F_{7/2}$), 1011 ($^4F_{9/2}\rightarrow{}^6F_{5/2}$), and 1172 nm ($^4F_{9/2}\rightarrow{}^6F_{3/2}$) are observed for $[Dy(NO_3)_3(bpm)_2]$ (Figure 6).

Sensitization of the ions that have an excited state at a lower energy and emit near-IR light also occurs. We reported previously that BPM could sensitize Nd^{III} luminescence in $[Nd(NO_3)_3(bpm)(CH_3OH)_2]$.[44] We have extended our work to the Yb^{III} and Er^{III} complexes. The emission spectrum of $[Yb(NO_3)_3(bpm)_2]$ displays the $^2F_{5/2}\rightarrow{}^2F_{7/2}$ transition with a maximum at 976 nm. Emission from the $^4I_{13/2}$ excited state of Er^{III} is also observed after excitation of BPM ($^4I_{13/2}\rightarrow{}^4I_{15/2}$ transition at 1550 nm), but its intensity is poor. For the Er complex, as for the Nd counterpart, weak phosphorescence from the BPM triplet state appears in the visible range of the emission spectrum (Figure 6). This is a consequence of the relatively high energy difference between the BPM triplet state and the emissive excited states of these ions. It amounts to approximately 12650, 13850 and 17640 cm^{-1} for the Nd^{III}, Yb^{III}, and Er^{III} complexes, respectively, assuming the 0-phonon transition of the BPM triplet state to be at 24100 cm^{-1} (415 nm).[44] These investigations point to the triplet-state energy of BPM and the resulting energy gap with respect to Ln receiving states being too large to minimize loss of energy by nonradiative deactivation pathways from the ligand states. Quantum yields of the Nd^{III} and Er^{III} complexes could not be measured because the emission intensity was too low. However, $[Yb(NO_3)_3$-

$(bpm)_2$] is quite luminescent with a quantum yield of 0.8%, which is comparable with that reported recently for trinuclear KAlYb and KYb2 helicates.[65] The greater luminescence intensity of Yb^{III} complexes than of Nd^{III} and Er^{III} complexes is usual and is due to the larger energy gap between their emissive level and the higher sublevel of the ground state.

Conclusions

Monometallic complexes formed between the trivalent lanthanide and uranyl ions and 2,2′-bipyrimidine and nitrate ions as ligands have been isolated and structurally characterized. All the compounds were found to be air-stable, but we have shown by X-ray crystallography that it is preferable to handle them in dehydrated solvents, as water can displace the ligand molecules. In addition, luminescence measurements in a undried coordinating solvent are consistent with decoordination of BPM at the concentrations usually used for photophysical studies. Bipyrimidine sensitizes the luminescence of visible- and NIR-emitting lanthanide ions, as well as of uranyl ions. Due to efficient BPM-to-metal energy transfers, the Eu, Tb, Dy, and Yb complexes display good aptitude for emitting red, green, yellow, and near-IR light in the solid state, respectively. In particular, quite large quantum yields are found for $[Ln(NO_3)_3(bpm)_2]$ complexes: 70.0% for Eu, 80.0% for Tb, 5.1% for Dy, and 0.8% for Yb. The values for Eu and Tb are among the highest reported to date for molecular complexes in the solid state. We also emphasize the fact that the same ligand, 2,2′-bipyrimidine, is able to sensitize the luminescence of several f-metal ions efficiently, which is not so usual: for energetic reasons; when a ligand transfers energy efficiently to one of these ions, the transfer to the other ions is less quantitative.

This work highlights two characteristics of BPM. First, as shown previously,[44–46,66a–c] it is versatile and able to act both as a terminal and as a bridging ligand for lanthanide ions. Secondly, BPM is a ligand of choice for the design of photoluminescent molecular edifices; we note especially that its role in the sensitization of the luminescence of several 4f-metal ions has not been recognized and investigated previously. Consequently, the reported complexes are potential building blocks for solid-state photoluminescent materials. Work is under way along these lines, to create new polymetallic architectures with predetermined photophysical properties.

Experimental Section

Materials and methods: 2,2′-Bipyrimidine, $Ce(NO_3)_3{\cdot}6H_2O$ (99.999%), $Nd(NO_3)_3{\cdot}H_2O$ (99.99%), $Sm(NO_3)_3{\cdot}6H_2O$ (99.999%), $Eu(NO_3)_3{\cdot}6H_2O$ hydrate (99.99%), $Gd(NO_3)_3{\cdot}6H_2O$ (99.99%), $Tb(NO_3)_3{\cdot}6H_2O$ (99.999%), $Dy(NO_3)_3{\cdot}6H_2O$ (99.9%), $Er(NO_3)_3{\cdot}5H_2O$ (99.9%), and $Yb(NO_3)_3{\cdot}5H_2O$ (99.9%) were purchased from Aldrich; $Tm(NO_3)_3{\cdot}6H_2O$ (99.99%) was purchased from Aesar; and $UO_2(NO_3)_2{\cdot}6H_2O$ was purchased from Prolabo. All chemicals were used as received. Solvents were dried by standard methods and distilled before use. The syntheses were performed under an inert atmosphere of argon. Elemental analyses were performed by Analytische Laboratorien at Lindlar (Germany) and the Service de Microanalyse, ICSN (Gif-sur-Yvette, France).

Synthesis of the complexes $[Ln(NO_3)_3(bpm)(MeOH)_2]$

Ln = Ce: A flask was charged with $Ce(NO_3)_3{\cdot}6H_2O$ (275 mg, 0.63 mmol) and BPM (100 mg, 0.63 mmol), and THF (10 mL) was condensed in it. After the mixture had been stirred for 2 h at 20°C, the white precipitate was filtered off and dried under vacuum. Crystallization from methanol gave colorless crystals of the MeOH solvate which afforded an off-white powder after drying under vacuum .Yield 220 mg (64%); elemental analysis: calcd (%) for $C_{10}H_{14}N_7O_{11}Ce$: C 21.90, H 2.57, N 17.88%; found: C 21.50, H 2.53, N 17.55.

Ln = Nd: The synthesis was as previously reported.[44]

Ln = Sm: The Sm derivative was prepared from $Sm(NO_3)_3{\cdot}6H_2O$ (281 mg, 0.63 mmol) and BPM (100 mg, 0.63 mmol) by the same procedure as for Ln = Ce. Yield 47%; elemental analysis: calcd (%) for $C_{10}H_{14}N_7O_{11}Sm$: C 21.50, H 2.53, N 17.55; found: C 21.55, H 2.69, N 17.39.

Synthesis of the complexes $[Ln(NO_3)_3(bpm)_2]{\cdot}THF$

Ln = Nd: An NMR tube was charged with $Nd(NO_3)_3{\cdot}6H_2O$ (21 mg, 48 μmol) and BPM (15 mg, 95 μmol), and THF (0.4 mL) was condensed in it. Pale purple crystals appeared within a few hours. Yield 22 mg (65%); elemental analysis: calcd (%) for $C_{20}H_{20}N_{11}O_{10}Nd$: C 33.43, H 2.80, N 21.44; found: C 33.47, H 2.61, N 21.21.

Ln = Sm: The colorless Sm derivative was prepared from $Sm(NO_3)_3{\cdot}6H_2O$ (21 mg, 47 μmol) and BPM (15 mg, 95 μmol) by the same procedure as for Ln = Nd. Yield 58%; elemental analysis: calcd (%) for $C_{20}H_{20}N_{11}O_{10}Sm$ (%): C 33.14, H 2.78, N 21.26; found: C 33.42, H 2.63, N 20.97.

Ln = Eu: The colorless Eu derivative was prepared from $Eu(NO_3)_3{\cdot}H_2O$ (20 mg, 47 μmol) and BPM (15 mg, 95 μmol) by the same procedure as for Ln = Nd. Yield 73%; elemental analysis: calcd (%) for $C_{20}H_{20}N_{11}O_{10}Eu$: C 33.06, H 2.77, N 21.21; found: C 33.45, H 2.81, N 21.16.

Ln = Tb: The colorless Tb derivative was prepared from $Tb(NO_3)_3{\cdot}6H_2O$ (338 mg, 0.75 mmol) and BPM (236 mg, 1.49 mmol) by the same procedure as for the $[Ln(NO_3)_3(bpm)(MeOH)_2]$ complexes. Yield 82%; elemental analysis: calcd for $C_{20}H_{20}N_{11}O_{10}Tb$ (%): C 32.76, H 2.75, N 21.01; found: C 32.89, H 2.82, N 20.93.

Ln = Er: Colorless crystals of the THF solvate of the Er derivative were obtained from $Er(NO_3)_3{\cdot}5H_2O$ (21 mg, 47 μmol) and BPM (15 mg, 95 μmol) by the same procedure as for Ln = Nd. These crystals were found to desolvate upon drying under vacuum to give an off-white powder. Yield 24 mg (68%); elemental analysis: calcd (%) for $C_{16}H_{12}N_{11}O_9Er$: C 28.70, H 1.81, N 23.01; found: C 28.35, H 2.02, N 22.41.

Ln = Yb: Crystals of the THF solvate of the Yb derivative were obtained from $Yb(NO_3)_3{\cdot}5H_2O$ (21 mg, 47 μmol) and BPM (15 mg, 95 μmol) by the same procedure as for Ln = Nd. Yield 71%; elemental analysis: calcd (%) for $C_{20}H_{20}N_{11}O_{10}Yb$: C 32.14, H 2.70, N 20.61; found: C 32.30, H 2.56, N 20.59.

Synthesis of the complexes $[Ln(NO_3)_3(bpm)_2]$

Ln = Eu: A flask was charged with $Eu(NO_3)_3{\cdot}6H_2O$ (100 mg, 0.24 mmol) and BPM (74 mg, 0.48 mmol), and THF (10 mL) was condensed in it. After the mixture had been stirred for 2 h at 20°C, the white precipitate was filtered off and dried under vacuum. Crystallization from MeOH gave colorless crystals of the compound. Yield 109 mg (63%); elemental analysis: calcd (%) for $C_{16}H_{12}N_{11}O_9Eu$: C 29.37, H 1.85, N 23.55; found: C 29.51, H 1.93, N 23.37.

Ln = Gd: The colorless Gd derivative was prepared from $Gd(NO_3)_3{\cdot}6H_2O$ (285 mg, 0.63 mmol) and BPM (200 mg, 1.26 mmol) by the same procedure as for Ln = Eu. Yield 63%; elemental analysis: calcd (%) for $C_{16}H_{12}N_{11}O_9Gd$: C 29.14, H 1.83, N 23.36; found: C 29.26, H 1.89, N 23.25.

Table 6. Crystal data and structure refinement details.

	$[Ce(NO_3)_3(bpm)(MeOH)_2]\cdot MeOH$	$[Sm(NO_3)_3(bpm)(MeOH)_2]\cdot MeOH$	$[Nd(NO_3)_3(bpm)_2]\cdot THF$	$[Sm(NO_3)_3(bpm)_2]\cdot THF$	$[Eu(NO_3)_3(bpm)_2]\cdot THF$
chemical formula	$C_{11}H_{18}CeN_7O_{12}$	$C_{11}H_{18}N_7O_{12}Sm$	$C_{20}H_{20}N_{11}NdO_{10}$	$C_{20}H_{20}N_{11}O_{10}Sm$	$C_{20}H_{20}EuN_{11}O_{10}$
M ($g\,mol^{-1}$)	580.44	590.67	718.71	724.82	726.43
crystal system	monoclinic	monoclinic	monoclinic	monoclinic	monoclinic
space group	$P2_1/n$ (No. 14)	$P2_1/n$ (No. 14)	$P2_1/c$ (No. 14)	$P2_1/c$ (No. 14)	$P2_1/c$ (No. 14)
a [Å]	8.3798(3)	8.3225(3)	9.6537(4)	9.6013(6)	9.6067(9)
b [Å]	15.6599(5)	15.5904(8)	14.7243(10)	14.7309(16)	14.721(3)
c [Å]	16.1249(6)	16.0338(8)	18.8929(13)	18.8015(18)	18.855(3)
α [°]	90	90	90	90	90
β [°]	104.867(2)	104.980(3)	95.158(4)	94.849(6)	95.286(9)
γ [°]	90	90	90	90	90
V [Å^3]	2045.18(13)	2009.70(16)	2674.6(3)	2649.7(4)	2655.1(7)
Z	4	4	4	4	4
ρ_{calcd} [$g\,cm^{-3}$]	1.885	1.952	1.785	1.817	1.817
μ ($Mo_{K\alpha}$) [mm^{-1}]	2.301	2.998	2.016	2.292	2.438
F(000)	1148	1164	1428	1436	1440
reflns collected	43194	45772	75554	67970	71410
independent reflections	3875	3810	5083	5001	5043
reflections observed [$I>2\sigma(I)$]	3499	3433	3900	3786	3240
R_{int}	0.026	0.035	0.036	0.043	0.071
parameters refined	283	283	379	379	379
$R1$	0.023	0.027	0.031	0.041	0.048
$wR2$	0.056	0.068	0.066	0.100	0.088
S	1.029	1.046	1.017	1.020	1.010
$\Delta\rho_{min}$ [$e\,Å^{-3}$]	−0.72	−1.19	−0.91	−0.67	−1.01
$\Delta\rho_{max}$ [$e\,Å^{-3}$]	0.39	0.64	0.62	1.49	0.78

Ln = Dy: The colorless Dy derivative was prepared from $Dy(NO_3)_3\cdot 6H_2O$ (220 mg, 0.63 mmol) and BPM (200 mg, 1.26 mmol) by the same procedure as for Ln = Eu. Yield 57%; elemental analysis: calcd (%) for $C_{16}H_{12}N_{11}O_9Dy$: C 28.91, H 1.82, N 23.17; found: C 28.69, H 1.94, N 22.83.

Ln = Tm: The colorless Tm derivative was prepared from $Tm(NO_3)_3\cdot 6H_2O$ (146 mg, 0.32 mmol) and BPM (100 mg, 0.63 mmol) by the same procedure as for Ln = Eu. Yield 85%; elemental analysis: calcd (%) for $C_{16}H_{12}N_{11}O_9Tm$: C 28.63, H 1.80, N 22.95; found: C 28.43, H 2.03, N 22.51.

Table 7. Crystal data and structure refinement details.

	$[Tb(NO_3)_3(bpm)_2]\cdot THF$	$[Er(NO_3)_3(bpm)_2]\cdot THF$	$[Yb(NO_3)_3(bpm)_2]\cdot THF$	$[Eu(NO_3)_3(bpm)_2]$	$[Gd(NO_3)_3(bpm)_2]$
chemical formula	$C_{20}H_{20}N_{11}O_{10}Tb$	$C_{20}H_{20}ErN_{11}O_{10}$	$C_{20}H_{20}N_{11}O_{10}Yb$	$C_{16}H_{12}EuN_{11}O_9$	$C_{16}H_{12}GdN_{11}O_9$
M ($g\,mol^{-1}$)	733.39	741.73	747.51	654.33	659.62
crystal system	monoclinic	monoclinic	monoclinic	monoclinic	monoclinic
space group	$P2_1/c$ (No. 14)	$P2_1/c$ (No. 14)	$P2_1/c$ (No. 14)	$P2_1/n$ (No. 14)	$P2_1/n$ (No. 14)
a [Å]	9.5630(5)	9.5171(2)	9.4951(4)	7.6772(2)	7.6729(6)
b [Å]	14.7363(9)	14.7326(5)	14.7411(7)	8.1744(4)	8.1854(4)
c [Å]	18.7503(15)	18.6603(6)	18.6405(6)	35.6064(18)	35.460(2)
α [°]	90	90	90	90	90
β [°]	94.726(5)	94.671(2)	94.700(3)	92.688(3)	92.583(4)
γ [°]	90	90	90	90	90
V [Å^3]	2633.4(3)	2607.70(13)	2600.30(19)	2232.08(17)	2224.8(2)
Z	4	4	4	4	4
ρ_{calcd} [$g\,cm^{-3}$]	1.850	1.889	1.909	1.947	1.969
μ ($Mo_{K\alpha}$) [mm^{-1}]	2.762	3.295	3.674	2.885	3.056
F(000)	1448	1460	1468	1280	1284
reflections collected	127155	75082	77993	66756	84885
independent reflections	4992	4950	4930	4222	4214
reflections observed [$I>2\sigma(I)$]	4397	4523	4389	3943	3715
R_{int}	0.046	0.021	0.053	0.023	0.027
parameters refined	379	379	379	334	334
$R1$	0.025	0.021	0.024	0.067	0.022
$wR2$	0.066	0.053	0.059	0.170	0.055
S	0.980	1.042	1.047	1.297	1.008
$\Delta\rho_{min}$ [$e\,Å^{-3}$]	−0.93	−1.12	−1.10	−2.49	−0.76
$\Delta\rho_{max}$ [$e\,Å^{-3}$]	0.49	0.68	0.66	2.84	1.12

Table 8. Crystal data and structure refinement details.

	$[Dy(NO_3)_3(bpm)_2]$	$[Tm(NO_3)_3(bpm)_2]$	$[Ce(NO_3)_2(bpm)(H_2O)_4]$ $[Ce(NO_3)_4(bpm)(H_2O)_2]$	$[Yb(NO_3)_2(bpm)(H_2O)_3]$ $[NO_3]\cdot bpm\cdot 4H_2O$	$[UO_2(NO_3)_2(bpm)]$
chemical formula	$C_{16}H_{12}DyN_{11}O_9$	$C_{16}H_{12}N_{11}O_9Tm$	$C_{16}H_{24}Ce_2N_{14}O_{24}$	$C_{16}H_{26}N_{11}O_{16}Yb$	$C_8H_6N_6O_8U$
M ($g\,mol^{-1}$)	664.87	671.30	1076.73	801.52	552.22
crystal system	monoclinic	monoclinic	triclinic	triclinic	orthorhombic
space group	$P2_1/n$ (No. 14)	$P2_1/n$ (No. 14)	$P\bar{1}$ (No. 2)	$P\bar{1}$ (No. 2)	$P2_12_12_1$ (No. 19)
a [Å]	7.6645(5)	7.6494(3)	9.0517(3)	10.9879(14)	9.0243(5)
b [Å]	8.1367(3)	8.1116(5)	13.9616(6)	12.3287(9)	11.8451(11)
c [Å]	35.416(2)	35.252(2)	14.0406(7)	12.5077(16)	12.7797(11)
α [°]	90	90	68.483(2)	62.619(7)	90
β [°]	92.812(3)	92.870(4)	86.462(3)	70.684(6)	90
γ [°]	90	90	85.515(3)	73.393(7)	90
V [$Å^3$]	2206.0(2)	2184.6(2)	1644.64(12)	1401.7(3)	1366.07(19)
Z	4	4	2	2	4
ρ_{calcd} [$g\,cm^{-3}$]	2.002	2.041	2.174	1.899	2.685
μ ($Mo_{K\alpha}$) [mm^{-1}]	3.463	4.138	2.852	3.430	11.939
F(000)	1292	1304	1052	794	1008
reflections collected	55664	55165	74053	37858	23622
independent reflections	4180	4136	6211	5320	2569
reflections observed [$I>2\sigma(I)$]	3634	3584	5495	4513	2501
R_{int}	0.038	0.036	0.023	0.062	0.075
parameters refined	334	334	505	397	209
$R1$	0.023	0.026	0.023	0.034	0.026
$wR2$	0.055	0.061	0.060	0.070	0.069
S	1.050	1.104	1.024	0.985	1.057
$\Delta\rho_{min}$ [$e\,Å^{-3}$]	−0.83	−1.08	−0.94	−1.27	−0.62
$\Delta\rho_{max}$ [$e\,Å^{-3}$]	0.81	0.67	0.66	0.69	1.17

Synthesis of $[UO_2(NO_3)_2(BPM)]$: A flask was charged with $UO_2(NO_3)_2\cdot 6H_2O$ (660 mg, 1.3 mmol) and BPM (206 mg, 1.3 mmol), and THF (50 mL) was condensed in it. The reaction mixture was stirred for 2 h at 20 °C. The volume of the yellow solution was reduced to ≈20 mL until a yellow solid was deposited on the walls of the flask. After filtration, slow diffusion of pentane into the solution led to the formation of yellow crystals. Yield 300 mg (42 %); elemental analysis: calcd (%) for $C_8H_8N_6O_8U$: C 17.34, H 1.45, N 15.16 %; found: C 17.46, H 1.13, N 15.42 %.

Crystallographic data collection and structure determination: The data were collected at 100(2) K on a Nonius Kappa-CCD area detector diffractometer[67] using graphite-monochromated $Mo_{K\alpha}$ radiation ($\lambda=$ 0.71073 Å). The crystals were introduced into glass capillaries with a protecting "Paratone-N" oil (Hampton Research) coating. The unit cell parameters were determined from ten frames, then refined on all data. The data (combinations of Φ and ω scans giving a complete data set up to $\theta=$ 25.7°) were processed with HKL2000.[68] The structures were solved by direct methods with SHELXS-97 and subsequent Fourier difference synthesis, except when an isostructural model was used as a starting point, and refined by full-matrix least-squares on F^2 with SHELXL-97.[69] Absorption effects were corrected empirically with the program SCALEPACK.[68] All non-hydrogen atoms were refined with anisotropic displacement parameters. When present, the hydrogen atoms bound to oxygen atoms were found on a Fourier difference map and all the others were introduced at calculated positions. All were treated as riding atoms with an isotropic displacement parameter equal to 1.2 (OH, CH, CH_2) or 1.5 (CH_3) times that of the parent atom. Crystal data and structure refinement parameters are given in Tables 6–8. The drawings were done with SHELXTL.[69]

Luminescence spectra: Solid-state measurements were performed on compounds conditioned as microcrystalline powders. The luminescence spectra were measured using a Horiba Jobin-Yvon Fluorolog-FL3-22 spectrofluorimeter, equipped with three-slit double-grating excitation and emission monochromators with dispersions of 2.1 $nm\,mm^{-1}$ (1200 grooves/mm). The steady-state luminescence was excited by unpolarized light from a 450 W xenon CW (continuous-wave) lamp and detected at an angle of 90° for dilute-solution measurements by a red-sensitive Hamamatsu R928 photomultiplier tube. The microcrystalline materials were analyzed with random orientation in a solid-state microholder with the front face detection at an angle of 22.5°. Spectra were reference corrected for both the excitation source light intensity variation (lamp and grating) and the emission spectral response (detector and grating). Uncorrected near-IR spectra were recorded using a liquid-nitrogen-cooled, solid indium/gallium/arsenic detector (850–1600 nm). Luminescence lifetimes (>30 μs) were obtained by pulsed excitation by using a FL-1040 UP xenon lamp. Luminescence decay curves were fitted by least-squares analysis by using Origin®. Quantum yield data were determined by an absolute method using a home-modified integrating sphere. The emission spectrum of $[UO_2(NO_3)_2(bpm)]$ was recorded on a Varian Cary Eclipse spectrophotometer.

Acknowledgements

Financial support from the Centre National de la Recherche Scientifique (CNRS) and the Commissariat à l'Energie Atomique (CEA) is gratefully acknowledged. J.C.B. and F.G. thank the Swiss National Science Foundation for support.

[1] A. Bencini, C. Benelli, A. Caneschi, R. L. Carlin, A. Dei, D. Gatteschi, *J. Am. Chem. Soc.* **1985**, *107*, 8128.
[2] C. Benelli, D. Gatteschi, *Chem. Rev.* **2002**, *102*, 2369.
[3] I. Hemmilä, T. Ståhlberg, P. Mottram, *Bioanalytical Applications of Labeling Technologies*, 2nd ed., Wallac Oy, Turku, **1995**.
[4] N. Weibel, L. J. Charbonnière, M. Guardigli, A. Roda, R. Ziessel, *J. Am. Chem. Soc.* **2004**, *126*, 4888.
[5] A. M. Reynolds, B. R. Sculimbrene, B. Imperiali, *Bioconjugate Chem.* **2008**, *19* , 588.
[6] E. Pazos, D. Torrecilla, M. V. López, L. Castedo, J. L. Mascareñas, A. Vidal, M. E. Vázquez, *J. Am. Chem. Soc.* **2008**, *130*, 9652.
[7] M. Tan, Z. Ye, G. Wang, J. Yuan, *Chem. Mater.* **2004**, *16*, 2494.
[8] M. A. Bacigalupo, G. Meroni, F. Secundo, R. Lelli, *Talanta*, **2008**, *77*, 126.

[9] M. F. Rega, J. C. Reed, M. Pellecchia, *Bioorg. Chem.* **2007**, *36*, 113.
[10] J.-C. G. Bünzli, *Chem. Lett.* **2009**, 210.
[11] T. Jüstel, H. Nikol, C. Ronda, *Angew. Chem.* **1998**, *110*, 3250; *Angew. Chem. Int. Ed.* **1998**, *37*, 3084.
[12] J. Hao, S. A. Studenikin, M. Cocivera, *J. Lumin.* **2001**, *93*, 313.
[13] A. de Bettencourt-Dias, *Dalton Trans.* **2007**, 2229.
[14] J. Kido, Y. Okamota, *Chem. Rev.* **2002**, *102*, 2357.
[15] T. Matsuzawa, Y. Aoki, T. Takeuchi, Y. Murayama, *J. Electrochem. Soc.* **1996**, *143*, 2670.
[16] J. E. Geusic, H. M. Marcos, L. G. van Uitert, *Appl. Phys. Lett.* **1964**, *4*, 182.
[17] Y. Guyot, H. Canibano, C. Goutaudier, A. Novoselov, A. Yoshikawa, T. Fukuda, G. Boulon, *Opt. Mater.* **2005**, *27*, 1658.
[18] K. Kuriki, Y. K. Okamoto, *Chem. Rev.* **2002**, *102*, 2347.
[19] A. Polman, F. C. J. M. van Veggel, *J. Opt. Soc. Am. B* **2004**, *21*, 871.
[20] G. C. Righini, C. Arnaud, S. Berneschi, M. Bettinelli, M. Brenci, A. Chiasera, P. Feron, M. Ferrari, M. Montagna, G. Nunzi Conti, S. Pelli, H. Portales, C. Siligardi, A. Speghini, L. Zampedri, *Opt. Mater.* **2005**, *27*, 1711.
[21] K. Driesen, C. Görller-Walrand, K. Binnemans, *Mater. Sci. Eng. C* **2001**, *18*, 255.
[22] V. Bekari, L. Panagiotis, *Adv. Mater.* **1998**, *10*, 1455.
[23] T. Jin, S. Tsutsumi, Y. Deguchi, K. I. Machida, G. Y. Adachi, *J. Electrochem. Soc.* **1995**, *142*, L195.
[24] O. A. Serra, E. J. Nassar, I. L. V. Rosa, *J. Lumin.* **1997**, *72*, 263.
[25] H. Li, S. Inoue, K. I. Machida, G. Y. Adachi, *Chem. Mater.* **1999**, *11*, 3171.
[26] P. Lenaerts, A. Storms, J. Mullens, J. D'Haen, C. Görller-Walrand, K. Binnemans, K. Driesen, *Chem. Mater.* **2005**, *17*, 5194.
[27] B. Yan, H. F. Lu, *Inorg. Chem.* **2008**, *47*, 5601.
[28] C. Janiak, *Dalton Trans.* **2003**, 2781.
[29] J. L. Belof, A. C. Stern, M. Eddaoudi, B. Space, *J. Am. Chem. Soc.* **2007**, *129*, 15202.
[30] T. K. Maji, S. Kitagawa, *Pure Appl. Chem.* **2007**, *79*, 2155.
[31] S. Kitagawa, R. Kitaura, S. I. Noro, *Angew. Chem.* **2004**, *116*, 2388; *Angew. Chem. Int. Ed.* **2004**, *43*, 2334.
[32] A. K. Cheetham, G. Férey, T. Loiseau, *Angew. Chem.* **1999**, *111*, 3466; *Angew. Chem. Int. Ed.* **1999**, *38*, 3268.
[33] B. Kesanli, W. Lin, *Coord. Chem. Rev.* **2003**, *246*, 305.
[34] L. X. Dai, *Angew. Chem.* **2004**, *116*, 5846; *Angew. Chem. Int. Ed.* **2004**, *43*, 5726.
[35] A. Nag, P. J. Schmidt, W. Schnick, *Chem. Mater.* **2006**, *18*, 5738.
[36] O. Guillou, C. Daiguebonne, "Lanthanide-containing coordination polymers," in *Handbook on the Physics and Chemistry of Rare Earths, Vol. 34* (Eds.: K. A. Gschneidner, J.-C. G. Bünzli, V. K. Pecharsky), Elsevier, New York, **2005**, pp. 359–404.
[37] C. L. Cahill, D. T. de Lill, M. Frisch, *CrystEngComm* **2007**, *9*, 15.
[38] Y. B. Dong, P. Wang, J. P. Ma, X. X. Zhao, H. Y. Wang, B. Tang, R. Q. Huang, *J. Am. Chem. Soc.* **2007**, *129*, 4872.
[39] J. M. Shi, W. Xu, Q. Y. Liu, F. L. Liu, Z. L. Huang, H. Lei, W. T. Yu, Q. Fang, *Chem. Commun.* **2002**, 756.
[40] A. de Bettencourt-Dias, *Inorg. Chem.* **2005**, *44*, 2734.
[41] C. Daiguebonne, N. Kerbellec, O. Guillou, J.-C. G. Bünzli, F. Gumy, L. Catala, T. Mallah, N. Audebrand, Y. Gérault, K. Bernot, G. Calvez, *Inorg. Chem.* **2008**, *47*, 3700.
[42] M. Frisch, C. L. Cahill, *Dalton Trans.* **2006**, 4679.
[43] Y. S. Jiang, Z. T. Yu, Z. L. Liao, G. H. Li, J. S. Chen, *Polyhedron* **2006**, *25*, 1359.
[44] G. Zucchi, O. Maury, P. Thuéry, M. Ephritikhine, *Inorg. Chem.* **2008**, *47*, 10398.
[45] A. Fratini, G. Richards, E. Larder, S. Swavey, *Inorg. Chem.* **2008**, *47*, 1030.
[46] V. Bekiari, K. A. Thiakou, C. P. Raptopoulou, S. P. Perlepes, P. Lianos, *J. Lumin.* **2008**, *128*, 481.
[47] S. A. Cotton, *Lanthanide and Actinide Chemistry*, Wiley, New York, **2006**.
[48] R. D. Shannon, *Acta Crystallogr. Sect. A* **1976**, *32*, 751.
[49] A. R. Al-Karaghouli, J. S. Wood, *Inorg. Chem.* **1972**, *11*, 2293.
[50] J. F. Bower, S. A. Cotton, J. Fawcett, D. R. Russell, *Acta Crystallogr. Sect. C* **2000**, *56*, e8.
[51] N. W. Alcock, D. J. Flanders, D. Brown, *Inorg. Chim. Acta* **1984**, *94*, 279.
[52] N. W. Alcock, D. J. Flanders, M. Pennington, D. Brown, *Acta Crystallogr. Sect. C* **1988**, *44*, 247.
[53] D. Visinescu, L. M. Toma, O. Fabelo, C. Ruiz-Pérez, F. Lloret, M. Julve, *Polyhedron* **2009**, *28*, 851.
[54] A. Trzesowska, R. Kruszynski, *Transition Met. Chem.* **2007**, *32*, 625.
[55] I. A. Charushnikova, C. Den Auwer, *Acta Crystallogr. Sect. E* **2004**, *60*, m1775.
[56] M. Fréchette, C. Bensimon, *Inorg. Chem.* **1995**, *34*, 3520.
[57] M. S. Grigoriev, C. Den Auwer, C. Madic, *Acta Crystallogr. Sect. E* **2001**, *57*, 1141.
[58] M. G. B. Drew, M. J. Hudson, P. B. Iveson, M. L. Russell, J. O. Liljenzin, M. Skiberg, L. Spjuth, C. Madic, *J. Chem. Soc. Dalton Trans.* **1998**, 2973.
[59] M. G. B. Drew, P. B. Iveson, M. J. Hudson, J. O. Liljenzin, L. Spjuth, P. Y. Cordier, A. Enarsson, C. Hill, C. Madic, *J. Chem. Soc. Dalton Trans.* **2000**, 821.
[60] a) M. Bredol, U. Kynast, C. Ronda, *Adv. Mater.* **1991**, *3*, 361; b) E. Brunet, O. Juanes, R. Sedano, J. C. Rodrigues-Ubis, *Photochem. Photobiol. Sci.* **2002**, *1*, 613.
[61] O. L. Malta, H. F. Brito, J. F. S. Menezes, F. R. Gonçalves e Silva, C. de Mello Donegá, S. Alves, Jr., *Chem. Phys. Lett.* **1998**, *282*, 233.
[62] A. Aebischer, F. Gumy, J.-C. G. Bünzli, *Phys. Chem. Chem. Phys.* **2009**, *11*, 1346.
[63] K. Driesen, R. Van Deun, C. Görller-Walrand, K. Binnemans, *Chem. Mater.* **2004**, *16*, 1531.
[64] K. Lunstroot, P. Nockemann, K. Van Hecke, L. Van Meervelt, C. Görller-Walrand, K. Binnemans, K. Driesen, *Inorg. Chem.* **2009**, *48*, 3018.
[65] M. Albrecht, R. Fröhlich, J.-C. G. Bünzli, A. Aebischer, F. Gumy, J. Hamacek, *J. Am. Chem. Soc.* **2007**, *129*, 14178.
[66] a) K. Kirschbaum, A. Fratini, S. Swavey, *Acta Crystallogr. Sect. C* **2006**, *62*, m186; b) A. Fratini, S. Swavey, *Inorg. Chem. Commun.* **2007**, *10*, 636; c) S. Swavey, J. A. Krause, D. Collins, D. D'Cunha, A. Fratini, *Polyhedron* **2008**, *27*, 1061.
[67] Kappa-CCD Software; Nonius BV, Delft, **1998**.
[68] Z. Otwinowski, W. Minor, *Methods Enzymol.* **1997**, *276*, 307.
[69] G. M. Sheldrick, *Acta Crystallogr. Sect. A* **2008**, *64*, 112.

Received: June 4, 2009
Published online: September 8, 2009

